Corrosion of Nitinol

Venugopalan, Trepanier

Proceedings of the Int'l Conference on Shape Memory and Superelastic Technologies
SMST-2000
(eds.) S. Russell, A. Pelton
pp. 261-270

2000

CORROSION OF NITINOL

Ramakrishna Venugopalan[1] and Christine Trepanier[2]

[1]*Department of Biomedical Engineering, University of Alabama at Birmingham*
1075 13th Street South, Hoehn 370, Birmingham, AL 35294-4461

[2]*Cordis Corporation—Nitinol Devices & Components*
47533 Westinghouse Drive, Fremont, CA 94539

ABSTRACT

Nitinol is a very attractive material for manufacturing minimally invasive therapy devices and tools because of its unique superelasticity and shape memory properties. While several studies have shown it possesses good biocompatibility, its high nickel content and possible dissolution during corrosion still remains a concern. However, electropolishing can significantly decrease nickel dissolution from Nitinol by forming a corrosion resistant titanium oxide surface layer. In general, electropolished Nitinol exhibits equivalent, if not better, static corrosion behavior and ability to resist and repassivate (repair) surface damage when compared to 316L stainless steel. Combining electropolished Nitinol with stainless steel, titanium, and tantalum does not significantly affect its corrosion behavior. However, combining electropolished Nitinol with gold, platinum, and platinum-iridium alloy can result in an order of magnitude increase in corrosion rate. Review of prior research indicates that nickel release from Nitinol decreases from well below dietary levels to nearly nondetectable levels in the first few days following immersion in a physiological media. Finally, review of prior *in vivo* studies indicate minimal corrosion of Nitinol during implantation with released nickel concentration in surrounding tissues or organs being equivalent to that released by 316L stainless steel.

INTRODUCTION

Nitinol (NiTi) is a very attractive material for minimally invasive therapy since it possesses unique mechanical properties (superelasticity and shape memory) and good biocompatibility [1]. In the last two decades, NiTi technology has contributed to significant improvements in orthopedics and orthodontics [2,3]. It is now overcoming the limits in designing smaller, more efficient minimally invasive tools and devices [4].

Although several studies have shown the good corrosion resistance and biocompatibility of NiTi, the high nickel content of the alloy (55 wt.% Ni) and its possible dissolution during corrosion still

remains a concern [5–9]. Tissues in the human body contain water, dissolved oxygen, proteins and various ions such as chloride and hydroxide and they present an aggressive environment to the metals or alloys used for implantation [10,11]. Thus every base-metal/alloy implanted in the body will corrode—it is a question of how much. Corrosion resistance of a metallic implant is thus an important aspect of its biocompatibility [12]. In addition to the release of ions in the physiological environment, the corrosion process will also result in the deterioration of dimensional parameters of the corroding body [13]. While large orthopedic implants like total hips and knees very rarely lose mechanical integrity purely due to corrosion fatigue, small and complex-geometry minimally invasive devices can be susceptible to failure due to mechanically assisted corrosion. Thus, when choosing a material for manufacturing minimally invasive devices, evaluation and optimization of the corrosion properties should be performed on samples representative of actual device surface finish or preferably the device itself.

In particular, NiTi corrosion behavior can be significantly improved after specific surface treatments such as electropolishing [14]. Not surprisingly, similar surface treatments are prescribed by the American Society for Testing and Materials (ASTM) to optimize the corrosion properties of stainless steel and other biomaterials (F86 standard) [15]. Electropolishing of NiTi homogenizes the thickness, topography and chemical composition of the surface layer by forming predominantly titanium oxide—a significant factor in improving corrosion resistance [16,17].

Still, most minimally invasive devices are susceptible to surface damage during their manipulation. Such damage can disrupt the surface layer and lead to significantly increased corrosion. Thus, the ability of the device to repair surface damage has to be ascertained in addition to determining the device's static corrosion behavior. Finally, galvanic corrosion may occur when dissimilar metals are coupled to NiTi. Indeed, different material devices could be placed in close proximity or a device may even be made from more than one material to take advantage of their specific properties. An example for the latter case is the use of noble metal markers on 316L Stainless Steel (SS) or NiTi devices to improve radiopacity.

Based on these considerations, the objectives of this paper are to: (1) discuss *in vitro* static corrosion behavior and repassivation ability of electropolished NiTi in comparison to electropolished SS, (2) discuss the *in vitro* galvanic corrosion behavior of electropolished NiTi in combination with other biomaterials, and (3) review prior research on nickel dissolution *in vitro* and *in vivo* corrosion of NiTi.

STATIC CORROSION BEHAVIOR—POTENDIODYNAMIC POLARIZATION TESTING

Potentiodynamic polarization testing was conducted on electropolished NiTi and SS discs to determine their individual corrosion behavior under static conditions in de-aerated Hank's solution at 37°C [18]. A generic schematic of experimental configuration used for corrosion testing is presented in Figure 1. After an hour of equilibration, polarization data were generated by conducting a forward scan from 100 mV more active than the corrosion potential (E_{corr}) to a threshold anodic current density of 10 mA/cm². The scan direction was reversed until the protection potential was achieved or the potential was 0 mV with reference to the E_{corr} Tafel extrapolation and Stern-Geary currents were used to calculate the corrosion current density (I_{corr}) in ampere/cm² at the E_{corr} (Par-Calc® Routine, Technical Notes/Software Manual, EG&G, Princeton Applied Research). The corrosion rate in mm/year (*CR*) was calculated based on equivalent weight and density values included in the experimental setup for the M352 software. The breakdown potential (E_{bd}) was determined
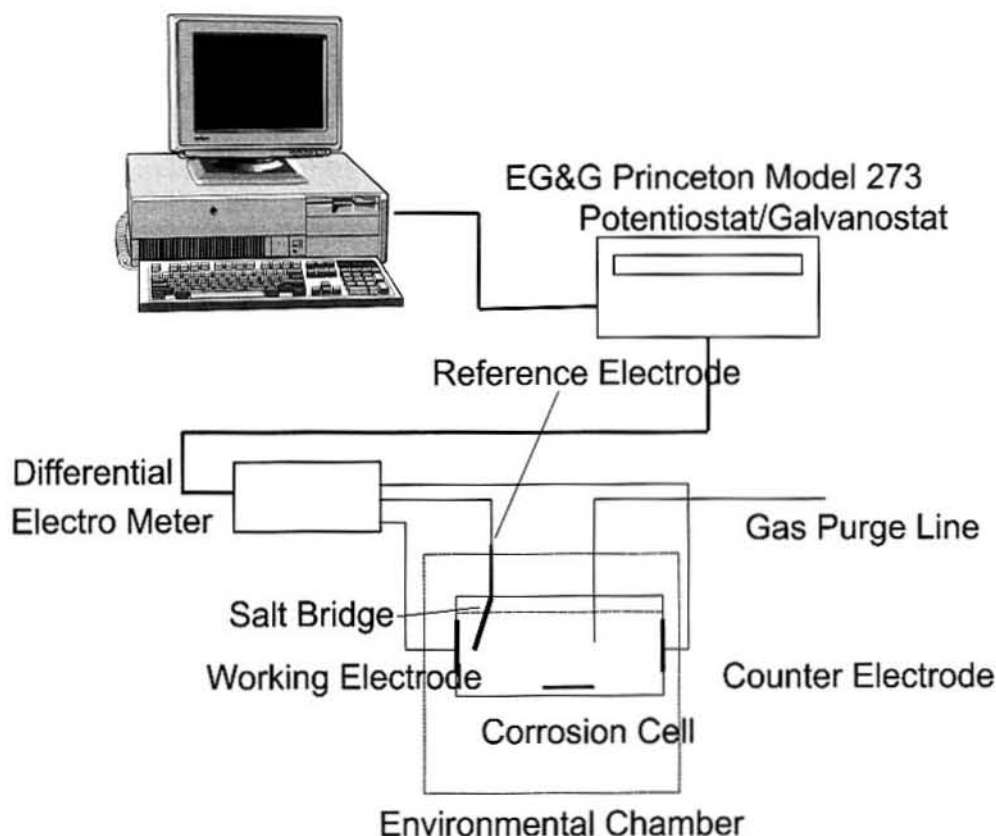
Figure 1 Generic schematic of experimental configuration used for corrosion testing.

from the y–axis coordinate corresponding to the intersection of a line-fit extrapolation of the passive and transpassive regions.

The E_{corr} is an indicator of the stability of surface condition. Thus, less variability in E_{corr} values from different samples is indicative of more consistent surface processing. The I_{corr} and calculated *CR* are relative measures of corrosion and illustrate how much of a material will be lost during the corrosion process. Hence, the higher the I_{corr} and calculated *CR*, the more the material lost. The E_{bd} is a measure of the region over which a surface layer is stable and corrosion resistant. Thus, a higher or more positive value of E_{bd} indicates a larger region of corrosion resistance.

Typical values of E_{corr}, I_{corr}, *CR*, and E_{bd} are presented in Table 1. Representative potentiodynamic polarization plots for NiTi and SS are presented in overlaid format in Figure 2. The E_{corr} for NiTi was more active than SS. The I_{corr} was very consistent and in the nA/cm^2 range for both NiTi and SS. The *CR* values also exhibited no significant difference between SS and NiTi. The E_{bd} for NiTi was almost three times greater than for SS. Prior research by Trepanier, et al. in 1998 [14] and Rondelli in 1996 [19] on comparative corrosion behavior of surface-modified NiTi also presented similar corrosion rates and breakdown potentials. Also, NiTi exhibited instantaneous repassivation on the reverse scan while SS exhibited a significant hysteresis. Hence, the SS was more susceptible to propagation of existing surface damage than NiTi.

Table 1 Potentiodynamic Polarization Test Results for NiTi and SS Discs in De-aerated Hank's Balanced Salt Solution. Values are Presented in Arithmetic Mean (Standard Deviation) Format. Superscript Letters in a Column Represent Groupings at a 95% Confidence Level.

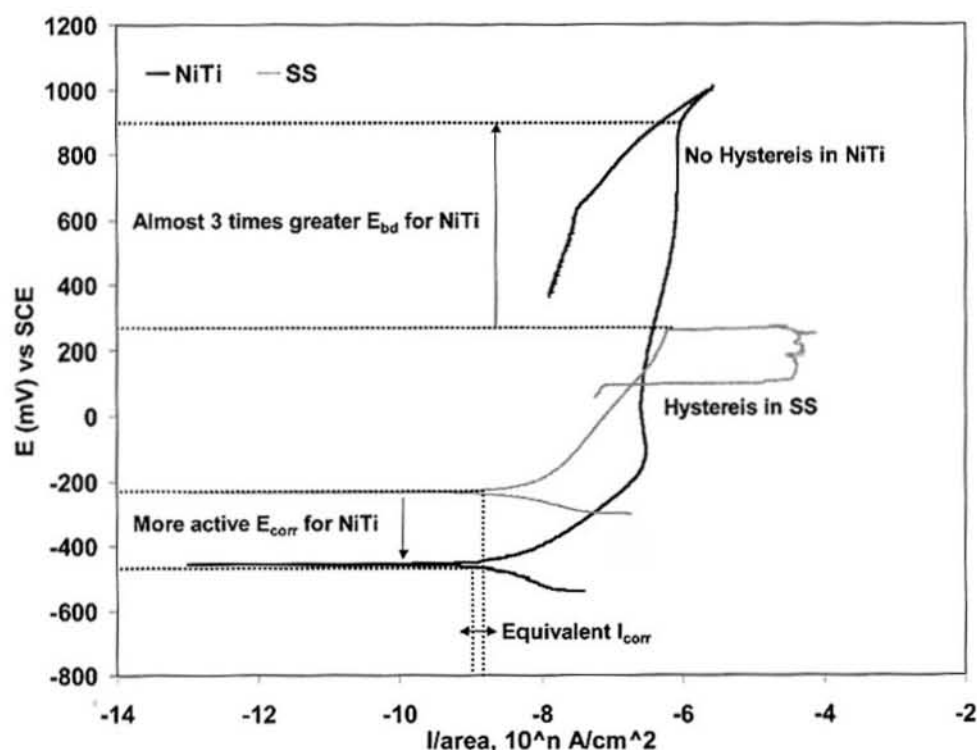| Sample Name	E_{corr} mV versus SCE	I_{corr} nAcm^{-2}	CR 10^{-5}mm/year	E_{bd} mV versus SCE
NiTi	−457(59)[a]	9(5)[a]	7.85(4.38)[a]	888(20)[a]
SS	−265(33)[b]	9(1)[a]	8.89(0.55)[a]	213(50)[b]

Figure 2 Representative cyclic polarization curves for NiTi and SS discs in de-aerated Hank's solution at 37 °C. Observe the equivalent corrosion rate and the larger passive or corrosion resistant region exhibited by NiTi.

REPASSIVATION ABILITY—POTENTIOSTATIC POLARIZATION TESTING

In order to determine their repassivation ability, electropolished NiTi and SS discs immersed in de-aerated Hank's media at 37°C were scratched using a diamond stylus across the whole exposed diameter 5 minutes before 0, 200, 400, and 600 mV potentiostatic holds [18]. The current flow during each 15-minute potentiostatic hold was monitored and normalized to sample surface area to obtain current density measurements. An asymptotically decreasing current density trend indicated

that the material was able to repassivate the scratch damage at that potentiostatic hold. An increasing current density trend indicated that the sample was not able to repassivate scratch damage at that potentiostatic hold. Current density greater than 500 $\mu A/cm^2$ was used as a threshold value to define total loss of ability of the material to repassivate [20].

Representative current density curves at 0, 200, 400 and 600 mV potentiostatic holds are presented in overlaid format in Figures 3a to d. NiTi and SS exhibited asymptotically decreasing current densities and repassivation after scratch damage at the 0 mV potentiostatic hold. NiTi exhibited asymptotically decreasing current densities and repassivation at the 200 mV potentiostatic hold. While the SS exhibited increasing current densities it still did not exceed the 500 $\mu A/cm^2$ current density threshold value. This behavior was indicative of a relatively less stable passive behavior by SS compared to NiTi at the 200 mV potentiostatic hold. At the 400 and 600 mV potentiostatic holds, both NiTi and SS exhibited increasing current densities that exceeded the 500 $\mu A/cm^2$ threshold value; indicative of total breakdown of passive layer. It should be noted that electropolished SS exhibited a faster current density transient past the 500 $\mu A/cm^2$ threshold value and also a few orders of magnitude higher corrosion rate than electropolished NiTi (Figures 3c and d). Thus, the region of repassivation capability after scratch damage for electropolished NiTi was at worst equivalent to and at best about 200 mV potential-range greater than electropolished SS.
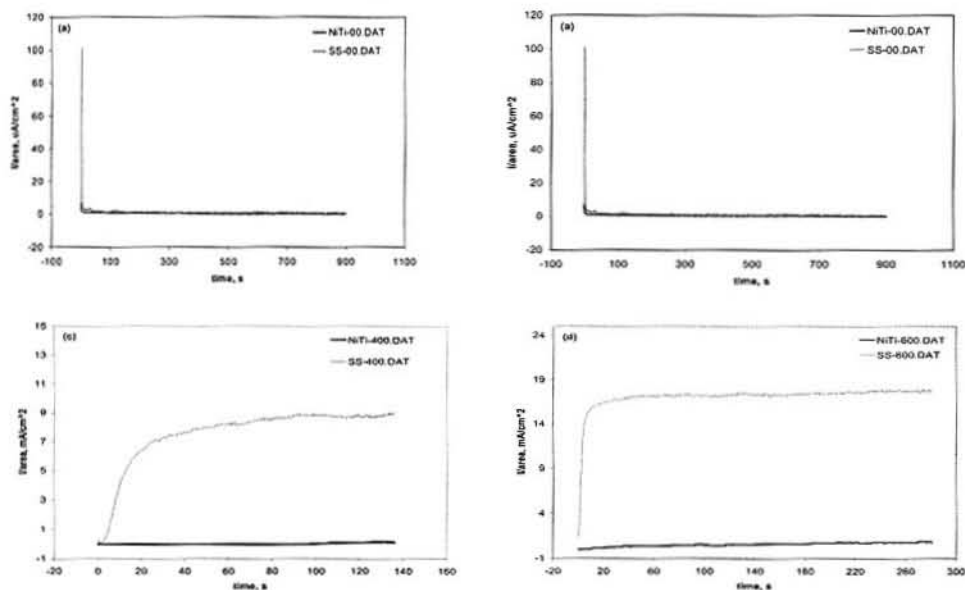

Figure 3 Representative scratch testing data curves for electropolished NiTi and SS in de-aerated Hank's solution at 37 °C. Current density profiles are presented for (a) 0 mV potentiostatic hold, (b) 200 mV potentiostatic hold, (c) 400 mV potentiostatic hold, and (d) 600 mV potentiostatic hold.

GALVANIC CORROSION BEHAVIOR

Disc samples of NiTi, platinum (Pt), platinum-iridium alloy (Pt-Ir), gold-palladium alloy (Au-Pd), SS, tantalum (Ta) and grade II titanium (Ti) were mechanically polished to 800 grit surface finish using SiC paper. NiTi and SS were electropolished. The other alloys were processed based on ASTM F86 protocols for surface preparation of metallic implants. Polarization curves (obtained per

protocol in the static corrosion section) for SS and Pt, Pt-Ir, Au-Pd, Ta and Ti were overlaid with an averaged NiTi curve for mixed-potential theory analysis [21]. The intersection of the cathodic portion of one curve and the anodic portion of the other curve was determined graphically (Figure 4). The y-axis intercept was the predicted coupled corrosion potential ($E_{couple-pre}$) and the x-axis intercept was the predicted coupled corrosion current density ($I_{couple-pre}$) for that combination [22].
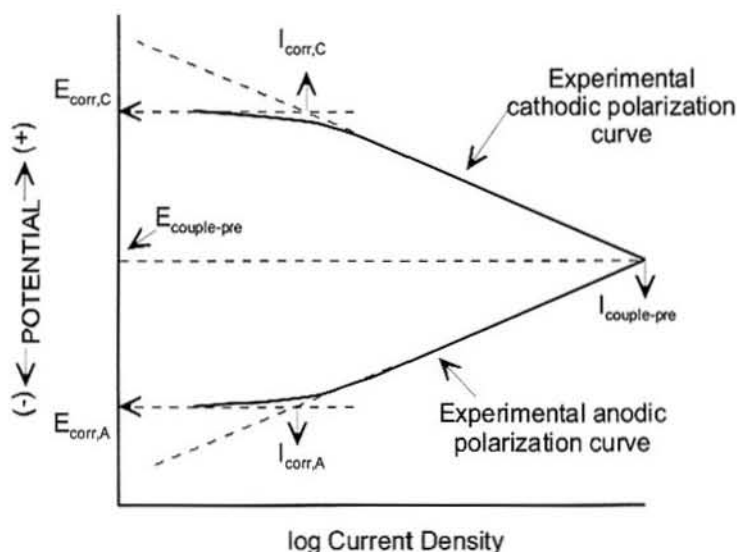

Figure 4 Schematic illustrating mixed-potential theory analysis.

The current-flow ($I_{couple-mes}$) that resulted when the six other materials were galvanically or directly coupled to NiTi alloy (cathode to anode ratio of 1:1) in de-aerated Hank's media at 37°C was measured using the potentiostat modified to perform as a zero-resistance ammeter (Technical Notes, EG&G, Oak Ridge, TN, 1991). Preliminary testing had determined that the current density measurements leveled out asymptotically after 6 hours. Hence the direct coupling tests were conducted for period of 12 hours. The current density value at t = 12 hours represents the asymptotic steady state value of the current flow after an extended period of galvanic coupling. This value may be the most relevant benchmark with reference to a galvanic corrosion scenario for implanted bimetallic devices [21].

The $E_{couple-pre}$ is indicative of the potential at which a device or a tool made by combining two different materials would rest. If this potential is within the region of corrosion resistance of the less corrosion resistant material or anode in the combination, the material combination will not force it to corrode at an accelerated rate. The $I_{couple-pre}$ and $I_{couple-mes}$ are the predicted and measured corrosion current density when two materials are combined, respectively. Thus, a higher coupled corrosion current density compared to individual-static-corrosion current density (I_{corr}) of the anode would indicate that it would corrode at an accelerated rate. The precision of corrosion measurements is a log decade or an order of magnitude [23]. Thus, only $I_{couple-mes}$ an order of magnitude greater than the I_{corr} can be considered a practically significant increase. Also, increasing the surface area of the cathode will make the combination more susceptible to galvanic corrosion phenomena.

Consolidated results from mixed-potential theory prediction and the direct coupling experiments are presented in Table 2. Mixed-potential theory calculations predicted that the galvanic coupling of NiTi to (a) Pt and Pt-Ir will result in $E_{couple\text{-}pre}$ in the middle of the passive region of the NiTi, (b) Au-Pd and SS will result in $E_{couple\text{-}pre}$ in the beginning of the passive region of the NiTi, and (c) Ta will result in $E_{couple\text{-}pre}$ similar to the corrosion potential of the NiTi. The $I_{couple\text{-}pre}$ for NiTi coupled to Pt, Pt-Ir and Au-Pd was greater than when coupled to Ta. The Tafel regions of NiTi and Ti were too close to each other to conduct tangential extrapolation using mixed-potential theory. The proximity of NiTi and Ti Tafel regions may be indicative of negligible galvanic influence on coupling. The predicted increase in the NiTi corrosion rate when coupled to SS was not conclusive due to significant standard deviation in the calculated results.

Table 2 Mixed-Potential Theory Predictions and Direct Coupling Results. Values are Presented in Arithmetic Mean (Standard Deviation) Format. Superscript Letters in a Column Represent Groupings at a 95% Confidence Level.

* Predictions Could Not be Made Due to Proximity of Tafel Regions

Cathode-Anode	Mixed-Potential Theory Prediction		Direct Coupling Experiments
	$E_{couple\text{-}pre}$ mV versus SCE	$I_{couple\text{-}pre}$ nAcm^{-2}	$I_{couple\text{-}mes}$ at t = 12 hours nAcm^{-2}
Pt-NiTi	126 (22)[a]	277 (9)	836 (74)[a]
PtIr-NiTi	40 (27)[b]	256 (3)	780 (302)[a]
AuPd-NiTi	−137 (3)[c]	285 (2)	608 (34)[a]
SS-NiTi	−218 (76)[d]	176 (111)	35 (5)[b]
Ta-NiTi	−406 (27)[e]	9 (6)	12 (17)[b]
Ti-NiTi	*	*	22 (17)[b]
Individual NiTi corrosion rate = 9 (5) nAcm^{-2}			

During direct coupling experiments, the largest $I_{couple\text{-}mes}$ were obtained for the noble alloys (Pt, Pt-Ir, Au-Pd) galvanically coupled to NiTi. The smallest $I_{couple\text{-}mes}$ values were obtained for SS, Ti and Ta galvanically coupled to NiTi. Also, the $I_{couple\text{-}mes}$ values for the (Pt, Pt-Ir, Au-Pd)/NiTi combinations were an order of magnitude greater than the values for the (SS, Ti, Ta)/NiTi combinations. Good rank order agreement was obtained between the predicted results from mixed-potential theory calculations and the results from direct coupling experiments. The increased coupled current density measurements obtained in this study were not of sufficient magnitude to breakdown the passivated NiTi surface layer due to galvanic action alone. Platt, et al. galvanically coupled SS to NiTi [24]. Their results did not indicate a statistically significant increase in current density due to galvanic coupling at a 1:1 cathode to anode ratio. However, they observed localized crevice corrosion phenomena occurring in the SS specimens while the NiTi specimens remained cathodic or protected. Thus, it is not possible to specifically isolate the galvanic corrosion effects from the crevice

corrosion effects for direct comparison to our study. They also observed an increase in galvanic activity when they reduced the surface area of the anode by 75%.

IN VITRO AND *IN VIVO* CORROSION

Since nickel release during the corrosion of NiTi is an important concern for its use as an implant material, several studies have measured this value. Barret, et al. [25] and Bishara, et al. [26] investigated nickel release from NiTi archwires (processed by the manufacturer) in saliva *in vitro* and reported that NiTi components released an average of 13.05 µg/day. This value is significantly below the estimated average dietary intake of 200 to 300 µg/day [25]. In a second study, orthodontic patients with NiTi appliances had nickel concentration in their blood measured over a period of 5 months [25]. Results showed no significant increase in the nickel blood level throughout this study.

A comparative *in vitro* cell culture study by Ryhanen, et al. measured nickel released from NiTi and SS in a fibroblast and osteoblast cell culture media [7]. Nickel levels were higher in the NiTi group the first day and decreased rapidly as a function of time to achieve similar levels as SS after 8 days in both media. Even though nickel release was higher in the NiTi group, cell proliferation or cell growth near the sample surface was not affected. Also, NiTi had been only mechanically polished while SS had been electropolished according to the guidelines of the manufacturer. Wever, et al. conducted a similar comparative study with passivated NiTi and SS in Hank's solution [8]. They also found that nickel release from NiTi was maximum the first day (14.5×10^{-7} µg/cm^{2}sec) and reached undetectable levels similar to SS after 10 days.

Castleman, et al. published the first *in vivo* biocompatibility data on NiTi. They implanted NiTi bone plates in the femurs of beagles for up to 17 months [27]. Retrieved plates exhibited no evidence of either localized or general corrosion. In addition, neutron activation analyses showed no metallic contamination of the surrounding tissues and organs for the NiTi sample group. A recent study by Ryhanen, et al. investigated implant surface corrosion and systemic trace metal release when NiTi and SS intramedullary rods were implanted in rats for up to 60 weeks [9]. Retrieval analyses exhibited no evidence of localized corrosion on the NiTi implants while apparent pits were observed on the SS control implants. Also, nickel content analysis of explanted organs did not indicate significant differences between NiTi and SS sample groups.

CONCLUSIONS

Electropolished Nitinol exhibits increased resistance to primary breakdown of the passive layer and an increased resistance to propagation of existing surface damage compared to 316L stainless steel under static conditions. Electropolished Nitinol also exhibits equivalent, if not better ability to repassivate surface damage compared to 316L stainless steel. The galvanic coupling to noble metals or alloys increases the corrosion rate of the electropolished Nitinol by two orders of magnitude, while coupling to the base-metal alloys resulted in a corrosion rate in the same order of magnitude as static uncoupled values. The increased current density measurements obtained during direct coupling experiments were not of sufficient magnitude to breakdown the electropolished Nitinol surface oxide layer. Review of prior research indicates that nickel release from Nitinol decreases from well below dietary levels to nearly nondetectable levels in the first few days following immersion in a physiological media. Finally, review of prior *in vivo* studies indicate minimal corrosion of Nitinol during implantation with released nickel concentration in surrounding tissues or organs being equivalent to that released by 316L stainless steel. Thus, carefully electropolished Nitinol is a very attractive material for manufacturing minimally invasive devices and tools.

ACKNOWLEDGEMENTS

REFERENCES

1. T.W. Duerig, A.R. Pelton, D. Stockel, *Bio-Medical Materials and Engineering* **6** (1996), 255-266.

2. J. Haasters, G. Salis-Solio, G. Bonsmann, in *Engineering aspects of shape memory alloys*, eds. T.W. Duerig, et al., (Jordan Hill, Oxford: Butterworth-Heinemann 1990), 426-444.

3. S. Lu. in *Engineering aspects of shape memory alloys*, eds. T.W. Duerig, et al., (Jordan Hill, Oxford: Butterworth-Heinemann 1990), 445-451.

4. T.G. Frank, et al., in *SMST-97: Proceedings of the Second International Conference on Shape Memory and Superelastic Technologies*, eds. A.R. Pelton, et al., (Pacific Grove, California: International Organization on the SMST, 1997), 509-514.

5. S.A. Shabalovskaya, *Bio-Medical Materials and Engineering* **6** (1996), 267-289.

6. C. Trepanier, et al., *JBMR (Appl Biomater)* **48** (1999), 165-171.

7. J. Ryhanen, et al., *JBMR* **35**, (1999), 451-457.

8. D.J. Wever, et al., *Biomat* **19** (1998), 761-769.

9. J. Ryhanen, et al., *JBMR* (in press).

10. L.L. Shrier, R.A. Jarman, G.T. Burstein, in *Corrosion – Metal/Environment Reactions, Third Edition*, (Jordan Hill, Oxford: Butterworth-Heineman, 1995), 2:3-2:164.

11. J.B. Park, R.S. Lakes, in *Biomaterials: An Introduction*, Second Edition, (New York: Plenum Press, 1992), 79-114.

12. J. Black, in *Biological Performance of Materials: Fundamentals of Biocompatibility*, Second Edition, (New York: Marcel Decker 1992), 38-60.

13. M.G. Fontana, in *Corrosion Engineering: Modern Theory and Applications, Third Edition,* (New York: MacGraw-Hill 1986), 445-502.

14. C. Trepanier, et al., *JBMR (Appl Biomater)* **43** (1998), 433-440.

15. ASTM F86, "Standard practice for surface preparation and marking of metallic surgical implants" in *Annual Book of ASTM Standards: Medical Devices and Services, Vol. 13.01.* (Philadelphia, PA: American Society for Testing and Materials, 1995), 6-8.

16. D.J. Wever, et al., *Biomat* **19** (1998), 761-769.

17. S. Trigwell, G. Selvaduray, in *SMST-97: Proceedings of the Second International Conference on Shape Memory and Superelastic Technologies*, eds. A.R. Pelton, et al., (Pacific Grove, California: International Organization on the SMST, 1997), 383-388.

18. R. Venugopalan, et al., 25th Annual Meeting of Society for Biomaterials/31st International Biomaterials Symposium, Providence, RI, 1999.

19. G. Rondelli. *Biomat* **17** (1996), (20): 2003-2008.

20. ASTM F746, "Standard test method for pitting or crevice corrosion of metallic surgical implant materials" in *Annual Book of ASTM Standards: Medical devices and Services, vol 13.01* (Philadelphia, PA: American Society for Testing and Materials, 1995), 192-197.

21. R. Venugopalan, et al., Submitted to World Biomaterials Congress, Kamuela, Hawaii, 2000.

22. D.A. Jones. *Principles and Prevention of Corrosion, Second Edition*, (Prentice Hall, Upper saddle River, NY), 1996: 168-198.

23. ASTM G61 "Standard test method for conducting cyclic potentiodynamic polarization measurements for localized corrosion susceptibility of iron-, nickel-, or cobalt-based alloys" in *Metals, Test Methods and Analytical Procedures, vol 03.02*. (Philadelphia, PA: American Society for Testing and Materials, 1995), 224-228.

24. J.A. Platt, et al., *Am J Orthod Dentofacial Orthop* **112** (1997), 69-79.

25. R.D. Barrett, S.E. Bishara, J.K. Quinn. *Am J Orthod Dentofac Orthop* **103** (1993), 8-14.

26. S.E. Bishara , R.D. Barrett , M.I. Selim. *Am J Orthod Dentofac Orthop* **103** (1993), 115-119.

27. L.S. Castleman, et al., *JBMR* **10** (1976), 695-731.